

# A Study on a Microwave-Driven Smart Material Actuator

Sang H. Choi<sup>\*a</sup>, Sang-Hyon Chu<sup>b</sup>, M. Kwak<sup>c</sup>, A. D. Cutler<sup>c</sup>

<sup>a</sup> NASA Langley Research Center, MS 188B, Hampton, VA 23681

<sup>b</sup> ICASE, NASA Langley Research Center

<sup>c</sup> Dept. of Mechanical Engineering, George Washington University

## ABSTRACT

NASA's Next Generation Space Telescope (NGST) has a large deployable, fragmented optical surface ( $\geq 8$  m in diameter) that requires autonomous correction of deployment misalignments and thermal effects. Its high and stringent resolution requirement imposes a great deal of challenge for optical correction. The threshold value for optical correction is dictated by  $\lambda/20$  (30 nm for NGST optics). Control of an adaptive optics array consisting of a large number of optical elements and smart material actuators is so complex that power distribution for activation and control of actuators must be done by other than hard-wired circuitry. The concept of microwave-driven smart actuators is envisioned as the best option to alleviate the complexity associated with hard-wiring. A microwave-driven actuator was studied to realize such a concept for future applications. Piezoelectric material was used as an actuator that shows dimensional change with high electric field. The actuators were coupled with microwave rectenna and tested to correlate the coupling effect of electromagnetic wave. In experiments, a  $3 \times 3$  rectenna patch array generated more than 50 volts which is a threshold voltage for 30-nm displacement of a single piezoelectric material. Overall, the test results indicate that the microwave-driven actuator concept can be adopted for NGST applications.

**Keywords:** microwave, actuator, piezoelectric, rectenna

## 1. INTRODUCTION

'Smart material' can be thought of as something that takes input energy in one form and converts it to output energy in another form.<sup>1</sup> Also, it responds to changes in its environment in predictable and pronounced ways.<sup>2</sup> These characteristics can be finely tuned for a wide variety of applications. One popular smart material is piezoelectric material that can produce displacement when an electric field is applied. It requires only relatively low power for operation and, as a result, the energy consumption and the need for thermal cooling can be minimized in applications in a real world.<sup>3</sup>

The piezoelectric actuator can be used in many applications such as adaptive surface of antenna or telescope. Recently, it was utilized in a surface compensation of inflatable reflector antenna,<sup>4</sup> and proved the surface compensation technique is extremely crucial to the success of NASA's future missions.<sup>5-8</sup> The Next Generation Space Telescope (NGST) is currently under development by NASA. The new telescope will replace the existing Hubble Space Telescope so that deep infrared and visible images of the most distant structures in our universe can be imaged and studied. The NGST will have a large segmented primary mirror ( $> 8$  m) that must be deployed and corrected in space using thousands of computer-controlled actuators. A large-sized optical reflector for images is vulnerable to structural deformation due to uneven thermal load, pre-existing stresses, or design flaws. Thus, the correction capability of the optical surface is necessary for precise images. The conventional approaches rely on the hard-wires for power and control of actuators. A hard-wired control circuit would be ideal for a simple system that is comprised of a few number of actuators. On the contrary, if the numerous nodal points (i.e., a thousand or more) of power and control are required, the hard-wire concept may present a serious complexity of wiring, the weight of wired network, the complexity of power and control networks, and the interdependency of power and control routines. The microwave-driven smart material actuator<sup>9</sup> is a new concept for actuators that are remotely controlled and power-fed, and autonomously activated without any hard-wired control routines. The interdependency of power and control routines, that might be inevitable for the hard-wired system because of networking many actuator elements, could be relaxed by loosely coupled microwave beam steering action and by beam-tailoring using microwave properties such as power, frequency, and polarization. Hence, the overall system that adopts microwave-driven actuators is exceedingly advantageous

<sup>\*</sup>Correspondence: Email: s.h.choi@larc.nasa.gov; Telephone: 757 864 1408; Fax: 757 864 7730

over the system with the conventional approaches. Power that activates the actuators can be wirelessly transmitted and converted into DC power using rectennas in this application. The rectenna (rectifier + antenna) which receives and converts microwave power into DC power is one of the key elements of this microwave-driven actuator concept.

Since the rectenna was first introduced by W. C. Brown in the 1960's,<sup>10</sup> it has been used for various applications such as microwave-powered helicopter,<sup>11</sup> the Solar Power Satellite (SPS)<sup>12</sup> that converts solar energy to RF and beams down to large 2.45-GHz rectennas on Earth, the 4.5-meter wingspan airplane that was powered only by microwave energy,<sup>13</sup> and the microwave-powered balloon for an electronically steerable phased array.<sup>14</sup> At first, a bulky bar-type dipole rectenna was developed<sup>15</sup> and then evolved to a planar thin-film type which rendered the large enhancement in the ratio of the weight to power output.<sup>16</sup> Also, another type of planar rectenna is the bow-tie antenna whose main advantages are simple design and broad-band impedance without the need of a separate low-pass filter.<sup>17,18</sup>

Recently, a lightweight patch rectenna was developed at NASA's Jet Propulsion Laboratory.<sup>19</sup> Its structure is composed of a square planar array of identical unit cells. Each cell contains a receiving antenna, filter and rectifier circuitry in its planar structure. Coupling between each copper antenna patch and its underlying filter and rectifier circuit occurs in two orthogonal slots in the copper ground plane. Hence, this scheme simplifies the design and construction of this rectenna patch. The array of the rectenna patches networked in a serial mode would provide a sufficient voltage that is required to drive actuators. Other factors that determine the performance of a rectenna patch are the parameters of a microwave source and the orientation of a rectenna patch at a far field. Three different approaches of rectenna-actuator combination were considered in the present study as follows:

#### **Single Module**

The single module consists of an actuator with a single rectenna integrated together as a single element. Two operational modes of a single module approach are envisioned. One is the case when a single rectenna patch is powerful enough to provide a sufficient voltage more than the threshold (i.e., 50 V in the NGST application) to an actuator. Otherwise, repetitive stroke is required for the case when the power from a single rectenna is not more than threshold value. For either a single or multiple stroke, rectenna performance is assumed to be optimized for microwave power, polarization, frequency, and a tailored patch design. For an example, the currently available rectenna patch which has a 60 % efficiency on 1 cm<sup>2</sup> area<sup>19</sup> would require at least a 1 W/cm<sup>2</sup> power density to provide more than 50 V. It is possible that a rectenna can be designed for a high voltage mode by adopting a high voltage breakdown (up to 15 volts) diode or a voltage boosting scheme or both. In this case, the microwave power density required for 50 volts output would be reduced by an order of magnitude. Or, a specially designed transmission antenna might be able to concentrate microwave within its diffraction limit to increase power density. For considering the actual NGST application (which requires a far-field coupling interaction) and the currently available rectenna and power density of microwave generators, the single module approach still imposes a great deal of challenge to achieve.

#### **Array of Rectenna Patches**

A single rectenna patch of approximately 1 cm<sup>2</sup> area that was designed for low voltage and high current power mode generates 5 V when it receives a 100 mW/cm<sup>2</sup> power density of microwave. A serial network of 20 rectenna patches of this kind would generate 100 V, which is fully adequate for actuator activation and control. The total receiving area would be 20 cm<sup>2</sup>, or 4.5 cm × 4.5 cm square. Any improvement of rectenna efficiency would reduce the number of patches in a network and the overall size of a networked array. An array of 20 rectennas with 80 % efficiency would require a 3.9 cm × 3.9 cm of square. With 20 rectennas of which diode has 15 volts breakdown voltage, at least 240 volts output is expected. If the output voltage required for an actuator is 120 volts, then the number of rectennas required will come down to 10. The size of the array is reduced to 3.16 cm × 3.16 cm. The size of a rectenna patch is also determined by microwave frequency. The above estimation of rectenna area was based on the frequency of 8.51 GHz.

#### **Distributed Control Logic Based Array Network**

This is not a patch array as discussed in the above. Each patch of rectenna embeds a control logic into it and is also networked to neighboring control-logic embedded patches. The networked control logic distributes or allocates power to a designated group of actuators whenever actuator controls are required.

A microwave transmission tends to disperse by its own nature. The power density received by rectenna patches may not be sufficient or less than the threshold requirement for mobilizing actuators due to the dispersion of microwave at a far-field area. In such a case, the networked control logic operates to allocate the power from individual patches elsewhere to the needed area. Hence, the power allocated to the needed area exceeds the threshold level. This approach utilizes most of microwave power that is incident on the rectenna patches and alleviates the requirements for pointing and concentration of

beam to achieve the power needed for a group of actuators. The power distribution to a designated group of actuators can be ordered by the external command signals that can be piggybacked on the principal waveband. Fig. 1 shows an illustration for networked array concept. A network circuitry that interconnects control logic of all participating rectennas allows a networked redistribution of power that is received by an individual rectenna of the array to a group of actuators from one location to another location. The networked redistribution of power can be implicitly interpreted as a process of the voltage amplification corresponding to the voltage needs for a group of actuators. The merits of this approach are the effective utilization of dispersive microwave field that is incident on a wide area and the tolerance of more degrees of freedom for control without regard to the location and gradient of incident energy.

In this study, the rectenna and multilayer piezoelectric actuator were not only separately tested at room temperature to characterize their properties on various conditions, but also combined to determine the response of a multilayer piezoelectric actuator to a power fed by a 3×3 rectenna patch.

## 2. EXPERIMENTAL

Test equipment was set up to prove and characterize the microwave-driven smart material actuator concept. Fig. 2 shows the schematic diagram for these tests. Hardware involved in our tests can be divided into three parts: 1) microwave generation and transmission, 2) rectenna and voltage measurement, and 3) smart actuator and displacement measurement. The microwave generation and transmission part is composed of a signal generator (2.0 - 26.0 GHz), a traveling wave tube (TWT) amplifier, and a feed horn antenna. Frequency and power level of microwave were set by the signal generator. The generated microwave was transmitted via a feed horn after it passed through the TWT amplifier. A patch rectenna fabricated at JPL was placed in the anechoic chamber to convert microwave into DC voltage. The DC voltage from rectennas was monitored by oscilloscope. The patch rectenna used in this study is composed of 9 unit cells, whose dimension is 1 cm × 1 cm, respectively. The 3×3 patch rectenna and its microstrip filter and rectifier circuit are shown in Fig. 3. In experiments, the patch rectenna was oriented for normal incidence and rotated 45° in azimuth so that both polarizations were illuminated via two orthogonal slots in each patch cell. In such configuration, the 3×3 patch rectenna has the overall effective area of 71.7 cm<sup>2</sup>. The received power by the patch rectenna could be calculated via multiplying the effective area of the patch rectenna by the power density that was measured using the microwave probe at a position of the rectenna.

In this study, DC power generated by rectenna was used as a power source to activate the multilayer piezoelectric actuator that is composed of PZT material. Multilayer piezoelectric actuators have been used for high longitudinal displacement, fast response, low driving voltage, and high energy conversion efficiency.<sup>20</sup> The typical properties of the multilayer piezoelectric actuator are listed in Table 1. The displacement of actuator was monitored using fiber-optic sensor system that provides a non-contacting measurement method. The fiber-optic sensor system in Fig. 4 is composed of a fiber-optic sensor, a low-pass filter, and an oscilloscope. The sensor measures the intensity of the light reflected from the moving surface of actuator and then converts this optical signal into a voltage output that linearly relates the tip-to-target distance. The low-pass filter is integrated into the measurement system for the output signal amplification. Also, the fiber-optic sensor system includes a function generator and a high voltage amplifier as a power source for smart actuators, for a general characterization.

## 3. RESULTS AND DISCUSSIONS

### 3.1. Smart Actuator

The multilayer piezoelectric actuator was tested using the independent power source with the fiber optic sensor system. We obtained the displacement-versus-voltage data with regard to various frequencies of AC voltage inputs: 0.5, 10, and 100 Hz. The magnitude of the applied voltage was described with a peak-to-peak value. The results are plotted in Fig. 5. As the frequency increases, the actuator showed a smaller displacement. If the displacement data are compared at the same voltage input, the expansion  $\Delta l$  at 50 V was 5.6, 5.1, and 4.1  $\mu\text{m}$  at 0.5, 10, and 100 Hz, respectively. In terms of  $d_{33}$  which is constant, or the strain coefficient along the applied electric field, the piezoelectric actuator exhibited 0.11, 0.10, and 0.08  $\mu\text{m}/\text{V}$  at each frequency. When the multilayer piezoelectric actuator was used, the displacement values exceeded the NGST requirement, 30 nm or  $\lambda/20$  ( $\lambda$  is the wavelength of the light) even in AC voltage cases. At high frequencies, the relative dielectric constant  $\epsilon_r$ , and the dissipation factor  $\tan \delta$  which is defined as the ratio of the effective series resistance to the effective series reactance are the factors that cause the dielectric losses. In general, piezoelectric materials dissipate energy in the form of heat, in proportion to the dissipation factor, the frequency, capacitance, and voltage.<sup>21</sup> As observed from the test

**Table 1.** Typical properties of the multilayer piezoelectric actuator.

<b>Mechanical</b>	
Dimension (L×W×H), mm	$5 \times 5 \times 18$
Compressive Strength, N/m <sup>2</sup>	$8.8 \times 10^8$
Tensile Strength, N/m <sup>2</sup>	$4.9 \times 10^6$
Young's Modulus, N/m <sup>2</sup>	$4.4 \times 10^{10}$
Density, kg/m <sup>3</sup>	7900
<b>Electrical</b>	
Capacitance, $\mu$ F	1.80

result, the displacement cannot be increased more than 7.5  $\mu$ m at 100 Hz, due to these effects (Fig. 5). In addition, the related temperature rise can cause the thermal expansion of the material and limit the power handling capability. But, in a static condition, virtually no heat is generated when voltage is applied.

### 3.2. Patch Rectenna

A JPL 3×3 patch rectenna was characterized for various conditions, such as transmitted power, frequency, beam incident angle, beam polarization. First, the effect of the transmitted power on voltage output and the power conversion efficiency was investigated with the rectenna that is placed at 15 in. away from the feed horn, while the frequency was set constant as 8.5 GHz. The power conversion efficiency,  $\eta$  is defined as follows:

$$\eta = \frac{\text{Output DC Power}}{\text{Received Microwave Power}} \quad (1)$$

The results show that voltage and the power conversion efficiency increase in both cases as the transmitted power increases. The rectenna works for a wide range of load resistors. The maximum voltage could be obtained for a given transmitted power when 100 k $\Omega$  was put in the circuitry (Fig. 6). In terms of the power conversion efficiency, 5.4 k $\Omega$  resistor case exhibited the best result (up to 52 %) (Fig. 7). However, 100,000 Ohm-loaded rectenna was used in all other tests to apply a high voltage to the actuator and maximize its performance. In this case, we obtained up to 73 V, whereas the efficiency was only 12 % (see Fig. 6). The loss by impedance mismatch causes the decrease in efficiency. The higher load resistor generates higher output voltage but widens the impedance mismatch of load coupling.

The frequency effect on rectenna performance was tested at a constant received power, 1.1 W, when the patch rectenna was placed at 25 in. away from the feed horn. The maximum voltage, 73 V was produced at 8.6 GHz as shown in Fig. 8. At a higher frequency, the voltage level tends to decrease to much smaller values.

DC power output can be controlled using two factors, transmitted power and frequency of microwave, without any change in the effective area of the patch rectenna. The effective area is dependent on incident angle and beam polarization. The effect of the incident angle on the voltage output is exhibited in Fig. 9. Likewise, the patch rectenna was 25 in. away from the feed horn, while the power and frequency of microwave was constant. The incident angle of 90° means that the patch rectenna is normal to the incident beam, while the incident angle of 0° indicates that it is parallel with the beam. As the incident angle decreased from 90° to 0°, the effective area is reduced and lowered the received power of the rectenna. As a result, the voltage output was decreased. It is interesting that  $\pm 30^\circ$  deviation from the normal position gave no clear reduction in the voltage output. A slightly noticeable amount of DC power could be observed even at the parallel position although the

effective area is theoretically zero. This result indicates that although the tests were conducted in an anechoic chamber beam reflection still existed.

In the patch rectenna, the polarization direction of microwave is very important for power transmission efficiency. Since the rectenna has two coupling slots that are orthogonal to each other, the rectenna rotated  $45^\circ$  in azimuth yields the maximum voltage output in our tests as shown in Fig. 10. Whereas  $\pm 15^\circ$  deviation from the optimal angle gave no large voltage difference, the minimum voltage occurred when illuminating only one slot at the polarization angle of  $0^\circ$ . The fact that DC power output from rectenna can be controlled by many factors as indicated above enables a wide degree of controllability for displacement of the smart actuators.

### 3.3. Microwave-driven Actuator

The multilayer piezoelectric actuator powered by the rectenna undergoes its displacement and was tested by controlling DC voltage output up to about 70 V (Fig. 11). From the results, we could obtain the nearly linear relationship between the displacement and the applied voltage as follows:

$$\Delta l = d_{33} V = 0.157 \cdot V \quad (2)$$

Therefore,  $d_{33}$  is  $0.157 \text{ } [\mu\text{m/V}]$  over a whole test range. At 50 V, the displacement was about  $8.0 \text{ } \mu\text{m}$ , which is much larger than the  $5.6 \text{ } \mu\text{m}$  that was obtained with the same level of AC voltage at 0.5 Hz. At this frequency, however, dielectric loss due to the high frequency is expected to be negligible. Thus, if rms value of AC voltage is considered instead of the peak-to-peak value, we obtain good agreement between the AC source at 0.5 Hz and the rectenna power, as shown in Fig. 11.

DC voltage application produces a short-term dimensional stabilization that is known as creep. Piezoelectric materials respond to a step change in the applied voltage, maintain their deformation for a desired time and then go back to their original state when the voltage is off. In the NGST application, the initial response behavior is more important, since any slow response of the smart actuators might cause trouble in getting a clear image at a necessary moment. Since the piezoelectric material is a capacitor as mentioned before, the activation of the piezoelectric material is similar to the injection of electric charges into a relative large capacitor. Therefore, a large electric current is needed to get a fast response from the actuator. The response time can be estimated with the following equation:

$$t = CV/i, \quad (3)$$

where  $C$  is the capacitance and  $i$  the drive current, and  $t$  the response time. The multilayer actuator used in our tests has a capacitance of  $1.8 \text{ } \mu\text{F}$ . According to the result plotted in Fig. 12, the DC power of the rectenna is able to drive the actuator with high-speed response at room temperature. Also, the experimental results give a reasonable agreement with the measured time, 100 msec, in creep test.

Some piezoelectric materials such as lithium niobate ( $\text{LiNbO}_3$ ) or lithium tantalate ( $\text{LiTaO}_3$ ) have a high  $C_T$ , temperature coefficient of delay (TCD), that is an indication of the frequency shift due to a change of temperature in electroacoustic applications. The higher the  $C_T$  is, the more the temperature-susceptibility is. In other words, a high  $C_T$  material behaves highly unstable and quickly reacts upon a temperature change. Thus, a high terminal voltage can be established at the pair of electrodes via the thermo-electrostatic charge effects. If a polarity of thermo-electrostatic charge is aligned with the polarity of a rectenna-created DC charge, the thermo-electrostatic charge becomes an additive to a rectenna-created DC charge.

Piezoelectric materials have high dielectric constants that indicate high susceptibilities. Therefore, when the piezoelectric material is placed within a microwave field, the piezoelectric material absorbs microwave energy by dielectric coupling and increases its own temperature within the piezoelectric crystal. The absorbed microwave energy changes the crystalline structure thermally and develops a capacitive charge in an electric field along the axis of polarization. The charge developed between electrodes is proportional to the absorbed energy and is inversely proportional to the crystal capacitance:

$$V_{TE} = \sum_{i=1}^N \left[ \sqrt{\frac{2 E_d}{C_s d_g}} \right], \quad (4)$$

where  $V_{TE}$  is the thermo-electrostatic charge voltage,  $E_d$  the thermal energy deposited in a piezoelectric crystal,  $C_s$  the static capacitance, and  $d_g$  the thickness of crystal or gap distance between electrodes. The summation notation of the above equation indicates the case of array formation. The crystal thickness determines the thermo-electrostatic charge voltage and bandwidth. Precisely speaking, the thermal diffusivity of material, which determines how fast energy is deposited in a crystal, is a determining factor for thickness and thermo-electrostatic charge power. For a microwave-driven actuator device, the thermal conductivity of material has a minor effect since the microwave absorption is evenly spread over the whole volume of dielectric medium, thus creating virtually no temperature gradients. Even though the energy is absorbed, the thermal conductivity of material and coupling coefficient reduce the absorbed energy for conversion.

Although the microwave-driven control concept can be applied to the smart actuators with success, it is not limited to them. More extensive applications of the remote power and control are possible in many areas such as microwave-driven membranes and strings, microwave-driven MEMS, and micro-robots for biomedical applications. Such applications of membranes and strings have large potential in inflatable antennas and telescopes, and mechanical configuration control of space structures. Moreover, rectennas can be adjusted to satisfy various special requirements of the specific applications. They can be used either for high voltage required for piezoelectric actuators or for high current required for magnetostrictive material actuators.

#### 4. CONCLUDING REMARKS

In this study, we proposed the novel concept of the microwave-driven smart actuator and investigated the feasibility of its possible application for future missions such as the NGST. The experimental results indicate that the multilayer piezoelectric actuator can be successfully utilized with a wide degree of controllability when the  $3 \times 3$  patch rectenna converts microwave energy to DC power that, in turn, drives the actuator. This concept eliminates the need for the hard-wiring of the smart actuators on the adaptive surfaces of the NGST or inflatable antenna. Hence, it could dramatically reduce the cost of distributed shape-control systems and find application in many future and technically challenging space missions. It is noted that all tests in this study were carried out at room temperature. Further study is needed to prove the concept in the cryogenic temperatures associated with the spacecraft environment, and to expose any problems that this environment may cause.

#### ACKNOWLEDGMENTS

This work was performed in cooperation with JPL's Transmitter Engineering Group and partially under the NASA contract (NAS1-97046, TA#380) to ICASE and the NASA grant (NCC1-217) to George Washington University.

#### REFERENCES

1. *1993 American Heritage College Dictionary*, 3rd edition (Houghton Mifflin).
2. I. V. Galaev, M. N. Gupta, and B. Mattiasson, "Use Smart Polymers for Bioseparations," *CHEMTECH*, No. 12, pp. 19-25, 1996.
3. J. Fanson and J. A. Garba, "Experimental Studies of Active Members in Control of Large Space Structure," *AIAA-ASME-ASCE-AHS 29th Structures, Structural Dyn. and Mat. Conf.*, pp. 9-17, Williamsburg VA, 1988.
4. T. K. Wu, "Piezoelectrically adjustable array for large reflector antenna surface distortion compensation," *Microwave and Optical Technology Letters*, Vol. 14, No. 4, pp. 221-224, 1997.
5. J. Huang, T. K. Wu, and S. W. Lee, "Tri-Band FSS with Circular Ring Elements," *IEEE Trans. Antennas Propagat.*, vol. AP-42, No. 2, pp. 166-175, 1994.
6. T. K. Wu, "Multiband FSS," in T. K. Wu (Ed.), *Frequency Selective and Grid Array*, John and Wiley & Sons, New York, 1995.
7. W. Schneider, J. Moore, T. Blankney, D. Smith, and J. Vacchione, "An Ultra-Lightweight High Gain Spacecraft Antenna," *IEEE Antennas Propagat. Int. Symp.*, Seattle, WA, June, pp. 886-889, 1994.
8. T. H. Lee, R. C. Rudduck, T. K. Wu, and C. Chandler, "Structure Scattering Analysis for SeaWinds Scatterometer Reflector Antenna Using Extended Aperture Integration and GTD," *IEEE Antennas propagat. Int. Symp.*, pp. 890-893, Seattle, WA, June, 1994.

9. Sang H. Choi, Lake, M., and Moore, C., "Microwave-driven Smart Material Actuators." Patent Pending, *NASA Case No. LAR 15754-1*, Feb 24, 1998.
10. W. C. Brown, et al., *U.S. Patent 3 434 678*, Mar. 25, 1969.
11. W. C. Brown, "Experiments involving a microwave beam to power and position a helicopter," *IEEE Trans. Aerosp. Electron. Syst.*, Vol. AES-5, No. 5, pp. 692-702, 1969.
12. W. C. Brown, "Solar Power Satellite Program Rev. DOE/NASA Satellite Power System Concept Develop. Evaluation Program," *Fianl Proc. Conf.* 800491, 1980.
13. J. Schlesak, A. Alden and T. Ohno, "A microwave powered high altitude platform," *IEEE MTT-S Int. Microwave Symp. Dig.*, pp. 283-286 1988.
14. W. C. Brown, "Design study for a ground microwave power transmission system for use with a high-altitude powered platform," *NASA Final Contractor Report 168344*, Raytheon Rpt. PT-6052, 1983.
15. W. C. Brown, "The history of power transmission by radio waves," *IEEE Trans. Microwave theory Tech.*, Vol. 32, No. 9, pp. 1230-1242, 1984.
16. W. C. Brown, "Performance characteristics of the thin-film, etched circuit rectenna," *IEEE MTT-S Int. Microwave Symp. Dig.*, pp. 365-367, 1984.
17. R. C. Compton, R. C. McPhedran, Z. Popovic, G. M. Rebeiz, P. P. Tong, and D. B. Rutledge, "Bow-Tie Antenna on a dielectric Half-Space: Theory and Experiment," *IEEE Trans. Antennas and Propagation*, Vol. AP-35, No. 6, pp. 622-631, 1987.
18. M. Tran and C. Nguyen, "A New Rectenna Circuit using A Bow-Tie Antenna for The Conversion of Microwave Power to DC Power," *Microwave and Optical Technology Letters*, Vol. 6, No. 11, pp. 655- 656, 1993.
19. NASA JPL, "Patch Rectenna for Converting Microwave to DC Power," *NASA Tech Briefs*, Vol. 21, January, p. 40, 1997.
20. K. Lubitz and H. Hellebrand, "Properties of PZT Multilayer Actuators," *IEEE 7th Inter. Symp. Applications of Ferroelectrics*, pp. 509-512, 1991.
21. IEEE, "IEEE Standard on Piezoelectricity," *IEEE/ANSI Std.*, 1978.

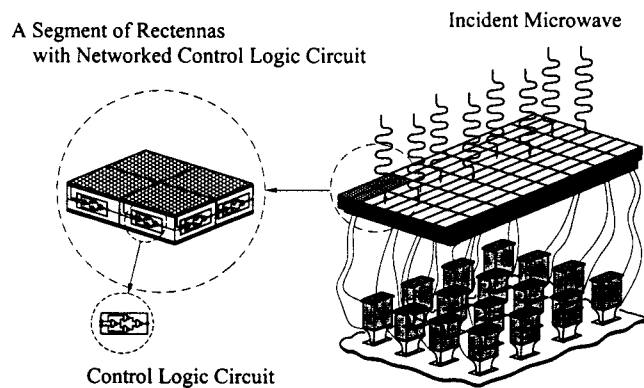


**Fig. 1.** A schematic diagram of networked control logic that is embedded into individual rectenna patch.

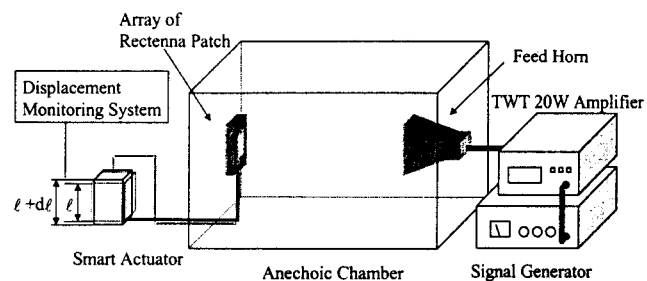
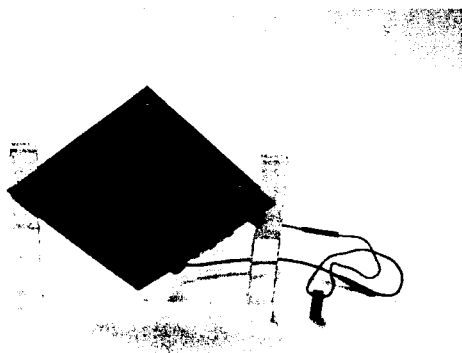
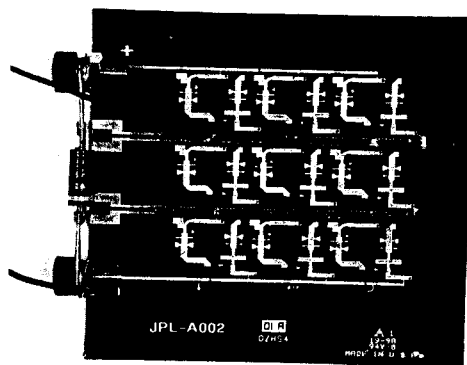


**Fig. 2.** Test setup for the microwave-driven smart material actuator.



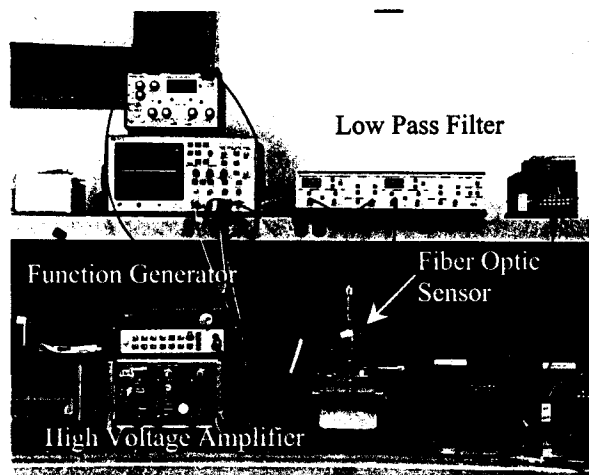
(a)



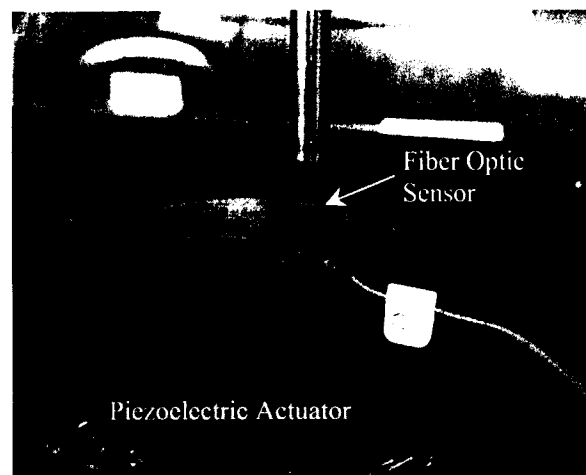
(b)

**Fig. 3.** The photograph of JPL 3x3 patch rectenna: (a) the rectenna with the multilayer piezoelectric actuator and (b) microstrip filter and rectifier circuit.





(a)



(b)

**Fig. 4.** The fiber optic sensor system that monitors the displacement of the piezoelectric actuator.

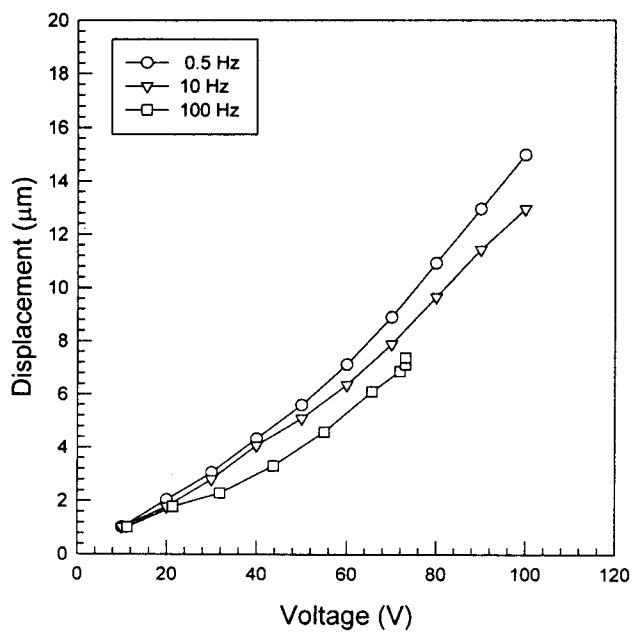


**Fig. 5.** AC Frequency effect on displacement of multilayer piezoelectric actuator with regard to voltage.

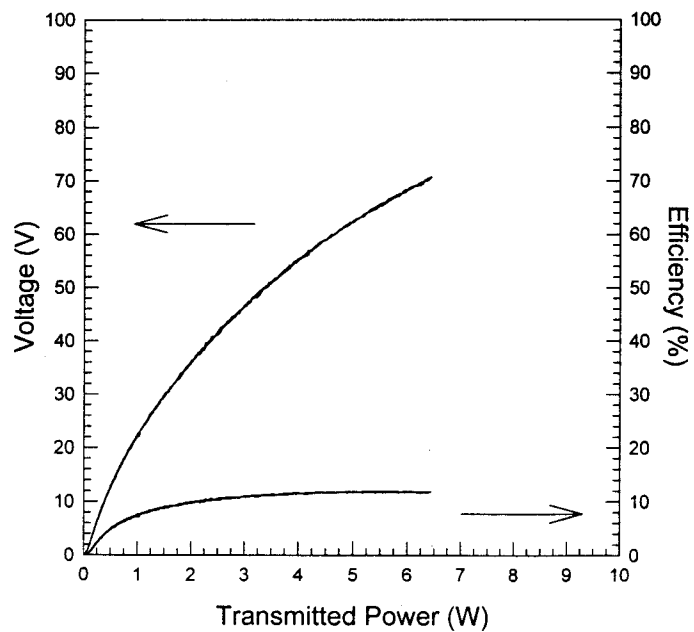


**Fig. 6.** Transmitted power effect on voltage output and efficiency obtained by 3x3 patch rectenna with 100,000 Ohm at 15" from feed horn at constant frequency of 8.5 GHz .

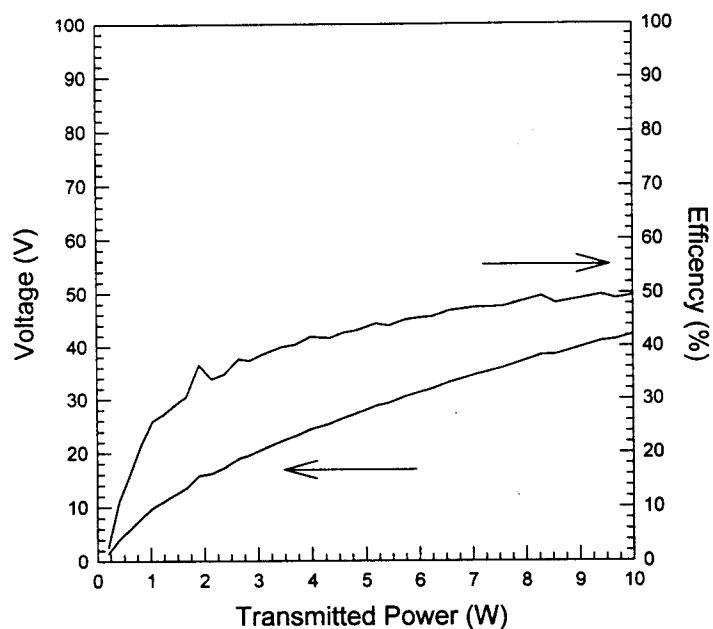


**Fig. 7.** Transmitted power effect on voltage output and efficiency obtained by 3x3 patch rectenna with 5,400 Ohm at 15" from feed horn at constant frequency of 8.5 GHz .

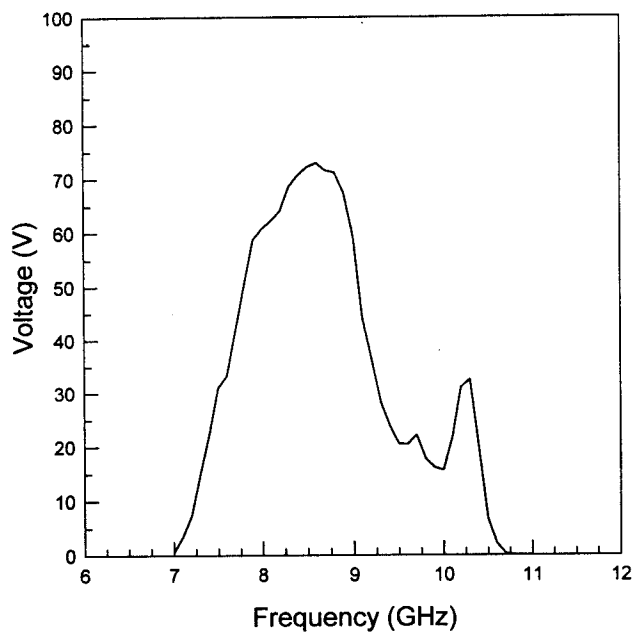


**Fig. 8.** Frequency effect on voltage output generated by 3x3 patch rectenna (100,000 Ohm) at 25" from feed horn with constant transmitted power of 1.1 W.

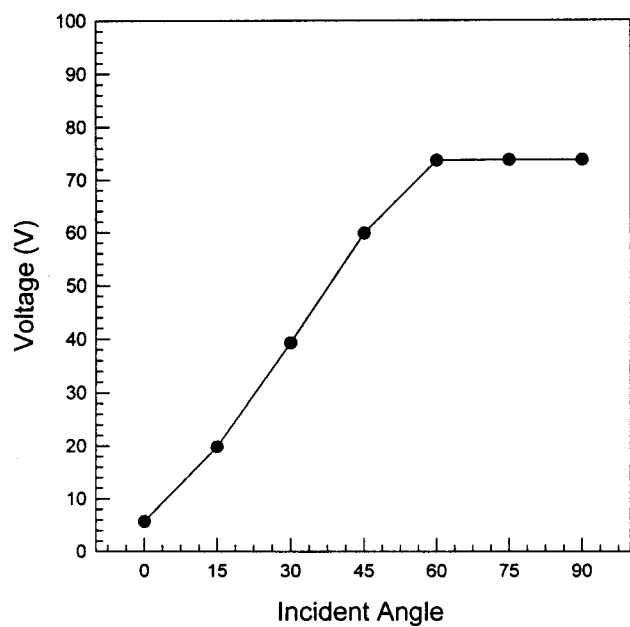


**Fig. 9.** The effect of incident angle of microwave on voltage output of 3x3 patch rectenna (100,000 Ohm) at 25" from feed horn with frequency of 8.6 GHz.

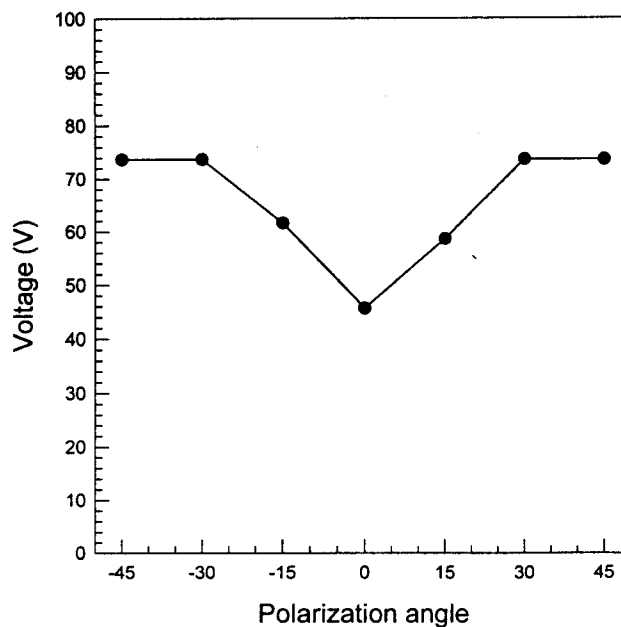


**Fig. 10.** The effect of polarization angle of microwave on voltage output of 3x3 patch rectenna (100,000 Ohm) at 25" from feed horn with frequency of 8.6 GHz.

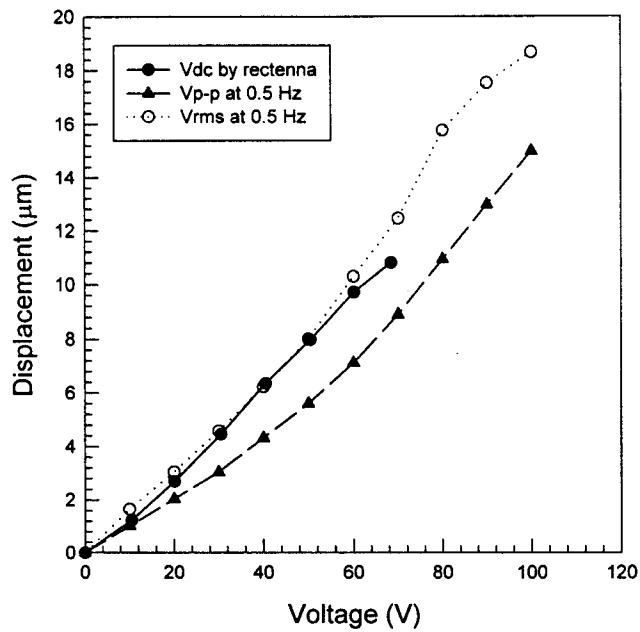


**Fig. 11.** Displacement of multilayer piezoelectric actuator activated by various power sources.

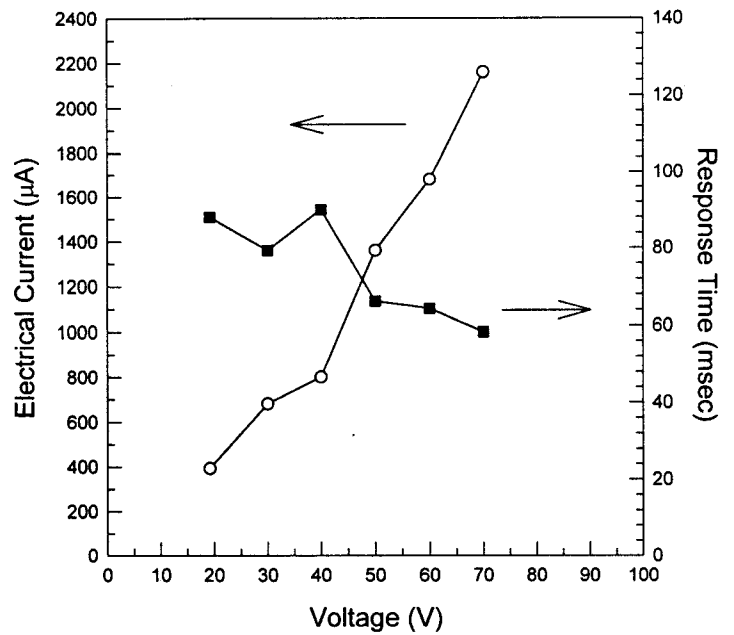


**Fig. 12.** Electrical current and response time with regard to voltage output produced by 3x3 patch rectenna.